






# Effects of Steam-Slaking on the Characteristics of Lime from Three Different UK Manufacturers

Cecilia Pesce<sup>1</sup>  , Martha C. Godina<sup>1</sup>, Alison Henry<sup>2</sup>, and Giovanni L. Pesce<sup>1</sup> 

<sup>1</sup> Department of Architecture and Built Environment, Northumbria University, Newcastle Upon Tyne NE1 8ST, UK

[cecilia.pesce@northumbria.ac.uk](mailto:cecilia.pesce@northumbria.ac.uk)

<sup>2</sup> Historic England, The Engine House, Fire Fly Avenue, Swindon SN2 2EH, UK

**Abstract.** The practice of producing lime mortars by slaking the quicklime directly in the sand rather than water is known as hot-mixing and, according to numerous historic accounts, was much more common in the past centuries than is generally appreciated by the majority of practitioners. During the last decade, a renewed interest has been dedicated toward the study of the hot-mixed mortar technology, as these mortars are regarded by most craftsmen of superior quality with respect to putty-based mortars in terms of workability, durability and other physical and mechanical properties. In such systems, the slaking of the quicklime is carried out by the moisture surrounding the sand grains and a small amount of added water. The steam developed by such initial slaking promotes further slaking which is supposed to be crucial in determining the characteristics of the lime, and, consequently, of the mortars. However, there are very few in-depth investigations regarding the role of steam on the characteristics of slaked lime. In this study, we have investigated the effects of steam slaking on the characteristics of lime produced by slaking the quicklime from three different UK manufacturers: Lhoist UK, Singleton Birch and Tarmac. Microstructural and mineralogical characteristics of the steam slaked limes are compared with those of the same limes slaked in excess of water and of the related oxides. Analyses were performed using X-ray fluorescence, scanning electron microscopy, and crystallite size and platelet abundance measured by X-ray diffraction data. The results provide useful information on the relations between the characteristics of the limestone used to produce the oxides and the effects of different slaking methods on the characteristics of the slaked lime. This can aid professional conservators to choose the right material and slaking method for the production of compatible mortars in conservation works.

**Keywords:** Lime · Steam slaking · Water slaking · Calcium oxide · Microstructure

## 1 Introduction

The hot-mixed mortar technology has seen a renewed interest over the last decade [1]. This type of mortar production entails mixing quicklime and sand together with a small amount of water. All water added to the mix is either consumed by hydration of the

quicklime or evaporates as steam. This creates a 'dry' mix. Once slaking is substantially complete, more water is added to produce a workable mortar. This procedure substantially differs from the procedure based on the use of lime putty, where the quicklime is first slaked in excess of water and the paste produced is only subsequently (sometimes even several years after) mixed with the aggregate to produce the mortar.

Hot-mixed mortars are of great interest to conservators and restoration practitioners, since the use of this technology was extremely common in the past centuries for the production of construction mortars and for plaster and render base coats. Hot-mixed mortars were cheaper and more practical to produce on site [2] and, according to some empirical record, outperform putty mortars in terms of stickiness, water retentivity, and workability. Increased mechanical properties and faster carbonation rate (with respect to putty mortars) have also been reported [3, 4].

In a recent work [5], we investigated some aspects of this technology that could explain the enhanced performance of the mortars. We started from the fact that, across the numerous reported variants of the procedure for hot-mixing, a common element is the fact the quicklime is initially slaked in a limited amount of water, before adding any water. This led us to infer that in such circumstance the quicklime is partially slaked by the moisture, first, and partially by the steam formed by the heat released as a result of the hydration reaction. Results of our study show that: (1) steam-slaked lime exhibits a different microstructure from the same lime slaked in an excess of water; (2) a mortar based on steam-slaked lime has a significantly higher water retention and lower water demand (i.e. it requires less water to reach an appropriate consistency) compared to a putty mortar. However, this study is limited to just one type of quicklime (i.e. produced by a single UK manufacturer).

It is generally known that limes sourced from different producers can have different properties due to differences in the geological properties of the limestone (across different quarries or even within the same quarry), calcination conditions, or other manufacturing processes [6]. In this work, we investigate the effects of the steam-slaking on the characteristics of slaked lime produced using three commercial quicklimes, provided by three UK manufacturers. The microstructure and mineralogy of both, the raw materials and the relative hydroxides obtained through water-slaking and steam-slaking are analysed and compared with those of the related oxides.

## 2 Methodology

### 2.1 Raw Materials

Commercial information on the three quicklimes used in the study are reported in Table 1 together with some information on the geology of the limestones used for their production. All quicklimes are classified as high calcium building limes according to the BS EN 459-1 [7]. Nominal granulometry varied from less than 0.180 mm for the Microlime (Singleton Birch) to less than 6 mm for the Calbux Fine 6 (Tarmac). Chemical composition of the quicklimes as determined by the X-ray fluorescence analysis is reported in Table 2 (details of the analysis in Sect. 82.3).

Table 1 highlights the fact that the limestones used by Tarmac and Lhoist share the same geological characteristics since they are extracted from quarries that are just 4

miles apart, located in the Bee Low limestone formation, in the Peak District, (Derbyshire). Limestones from the Bee Low formation are grey coloured, fine-to medium-grained calcarenites, mainly biosparites (i.e. the cement is composed of sparry calcite: clean, coarse-grained calcite crystals) and bioclasts (i.e. shell fragments and skeletons of microorganisms) [8]. The quicklime from Singleton Birch, instead, is produced with limestone extracted from the Melton Ross quarry (North Lincolnshire), in the Welton Chalk geological formation. Limestones originating in this formation are described as white, thickly bedded chalk with common flint (siliceous) nodules [9].

**Table 1.** Characteristics of the quicklime from each selected producer.

Producer	Product	Lime type	Nominal granulometry	Source	Geology
Tarmac	Calbux fine 6	CL90	≤6 mm	Tunstead quarry, Buxton (Derbyshire) [10, 11]	Bee low limestone formation (Carboniferous), highly pure calcarenite [12]
Lhoist UK	Milled quicklime	CL90	<2 mm	Brierlow quarry, Buxton (Derbyshire) [13]	
Singleton Birch	Microlime 90	CL90	≤0.18 mm	Melton Ross quarry, Melton Ross (North Lincolnshire) [14]	Welton chalk formation (cretaceous), biocalcarenite [12]

## 2.2 Slaking Process

The quicklimes tested in the project were used as received soon after delivery to the laboratory and slaked using two methods: with water and with steam, as described below.

**Water slaking.** A sample of 333 g of each quicklime, in thermal equilibrium with the laboratory temperature (20 °C), was placed in a metal container, where 1 L of degassed de-ionised water (also at 20 °C) was subsequently added, so that the CaO:H<sub>2</sub>O mass ratio was 1:3. The lime was, then, thoroughly mixed to promote hydration and, then, left to rest in water at 20 °C for 1 h. At the end of the slaking process, three samples of 5 g each were collected from each batch, dried for 6 h in a vacuum oven, and stored in a desiccator for analysis.

**Steam slaking.** A sample of 100 g of each quicklime was sieved to obtain particles with diameter 0.5 mm. Each sample was placed in an inert PTFE container. The containers were placed in a perforated steamer resting on a pan filled with de-gassed water. The steamer was, then, placed in an oven at 90 °C for 8 h to allow the steam generated

to slake the quicklime. The temperature inside the oven was regularly monitored using a thermocouple and adjusted throughout the test to maintain the water temperature at about 90 °C. At the end of the test, the temperature inside the oven was gradually reduced to room temperature. Subsequently, three samples of 5 g each were collected from each batch and dried in a desiccator for at least 24 h prior to analysis.

### 2.3 Analytical Techniques

The chemical composition of the quicklimes was determined by quantitative X-ray fluorescence (XRF), performed using a Spectro Xepos benchtop XRF analyser. The ‘Geochemistry traces’ method was used as internal calibration, and each analysis consisted of 4 passes: (i) atmosphere air; voltage 45.1 keV; (ii) atmosphere air; voltage 60.1 keV; (iii) atmosphere helium; voltage 22.5keV; (iv) atmosphere helium, Voltage 22.5keV. Resolution was 131.5eV at 5.89keV. Pressed pellets with a mixture of CaO and an inert wax binder (Fluxana Cereox wax, C<sub>38</sub>H<sub>76</sub>O<sub>2</sub>N<sub>2</sub>) were produced for analysis to improve consistency of the results.

The micro-morphological characterization of the oxides and hydroxides (both steam- and water-slaked) was carried out using a Tescan Mira 3 scanning electron microscope (SEM) in high vacuum mode, voltage at the gun 10 kV. Prior to analysis, the samples were coated with a 5 nm thick platinum layer.

Mineralogical characteristics were investigated using a Rigaku SmartLab X-ray diffractometer (Cu-K<sub>α</sub> radiation, parallel beam geometry, 2-θ range 10–90°, step 0.05°, scan speed 1.5°/min, 40 kV, 50 mA). Data evaluation (i.e. phase identification and crystallite size) was carried out using the Rigaku SmartLab Studio II software. Crystallite size was calculated using the Halder-Wagner equation [15].

## 3 Results and Discussion

### 3.1 Quicklime Composition

The results of the XRF analysis for all quicklimes are shown in Table 2.

Results show that all three quicklimes have a high calcium content (purity > 98%). However, Tarmac’s has a slightly reduced CaO content compared to the other products, and shows small traces of magnesium, silicon, and aluminum (these elements in Lhoist and Singleton Birch quicklimes are below level of quantification). Singleton Birch’s quicklime shows a slightly higher Fe<sub>2</sub>O<sub>3</sub> content compared to the other samples, although still a very small amount.

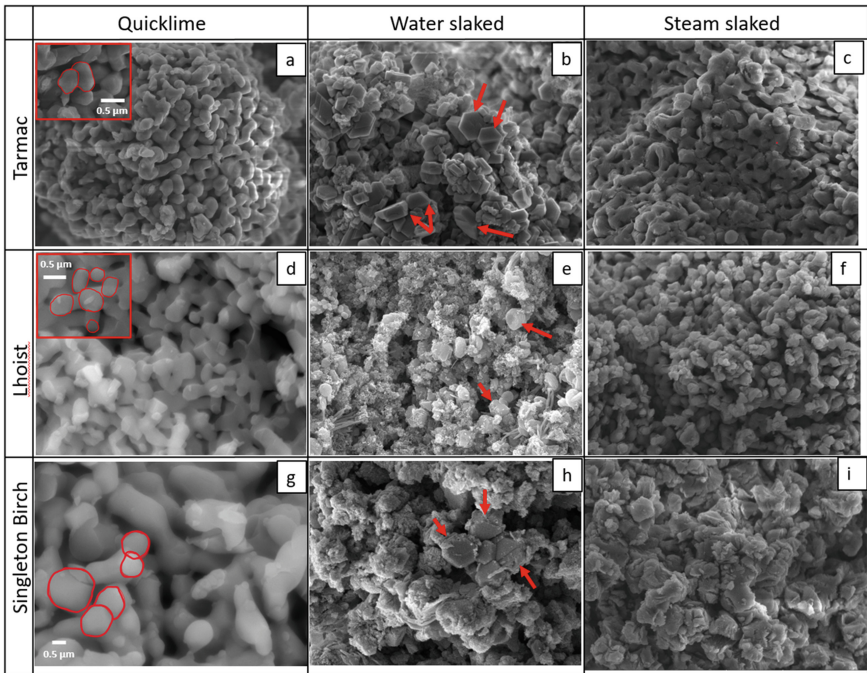
### 3.2 SEM Analysis

SEM micrographs of the quicklime, water-slaked lime and steam-slaked lime from each producer are shown in Fig. 1.

The quicklimes show the typical micromorphology of calcined calcium carbonate, i.e. agglomerates made of a network of interconnected round sub-particles [16]. The microstructure of Lhoist and Tarmac quicklimes are similar, with diameter of the

**Table 2.** Chemical composition of the quicklimes determined by XRF. Values marked with a (\*) are below level of quantification.

Phase	Tarmac	Lhoist	Singleton Birch
CaO	98.8	99.9	99.7
MgO	0.530	<0.017*	<0.017*
SiO <sub>2</sub>	0.361	<0.0011*	<0.0011*
Al <sub>2</sub> O <sub>3</sub>	0.083	<0.0038*	<0.0038*
Fe <sub>2</sub> O <sub>3</sub>	0.075	0.057	0.124
S	0.050	<0.001*	<0.001*
Cl	0.015	<0.003*	<0.003*
P <sub>2</sub> O <sub>5</sub>	0.009	<0.0007*	<0.0007*

**Fig. 1.** SEM micrographs of quicklime, water-slaked hydroxide, and steam-slaked hydroxide of each selected producer. View field of all micrographs is 10  $\mu\text{m}$ . The features measured in the quicklime are highlighted in insets in (a, d, g). In (b, e, h) well-developed hexagonal portlandite crystals are highlighted by the arrows.

sub-particles in the range 0.4–0.7  $\mu\text{m}$  (Fig. 2a, d), whereas Singleton Birch quicklime displays a significantly coarser microstructure, with diameter of the features in the range 0.8–1.5  $\mu\text{m}$  (Fig. 2g). It is worth noting that the textural features of the quicklime do not

necessarily reflect the granulometry of the product. Indeed, Tarmac and Lhoist quicklimes are made of particles with diameter up to 6 and 2 mm, respectively. However, under the SEM, they show a finer microstructure than the Singleton Birch quicklime which is made of finer granules (up to 0.18 mm) but shows a coarser microstructure under the microscope. Such textural difference between quicklimes is likely to be due to the different microstructure of the parent limestones.

The microstructure of the water-slaked limes are characterised by the presence of several well-developed equi-axed/short hexagonal portlandite crystals (with width up to 0.7  $\mu\text{m}$  for Lhoist and 1.5 for Tarmac and Singleton Birch) embedded in a matrix of nanometric, granular-shaped crystals. The slightly bigger crystals observed in the Tarmac and Singleton Birch quicklime in comparison with Lhoist may be linked with a higher reactivity of the Lhoist quicklime, as an increased reaction kinetics often promotes the formation of smaller crystals [17].

The steam-slaked limes display a distinctly different microstructure compared to the water-slaked limes. The microstructure of the steam-slaked samples resembles that of the parent quicklime, i.e. made of agglomerates of interconnected, rounded sub-particles stacked together (the full conversion of the oxide into hydroxide is confirmed by XRD analysis; see Sect. 82.3). This type of microstructure has been previously observed by the authors in steam-slaked Tarmac lime [5, 18]. At higher magnification, it is possible to observe that the particles display the hexagonal geometry typical of portlandite (Fig. 2). The observed microstructure is probably related to the fact that, when lime is slaked by steam, the hydration reaction occurs on a gas/solid interface, resulting in piles of thin platelets of portlandite stacked along the  $c$  axis [5, 19, 20]. This type of crystal growth results in mechanical stress in the newly-formed portlandite crystals [5], which exhibit nano-cracks on their surface (Fig. 2b). The size of the sub-particles slightly varies across producers. Similarly to what observed in the water-slaked limes, Tarmac and Singleton Birch samples show slightly bigger crystals (up to 0.7  $\mu\text{m}$ ) than Lhoist (up to 0.4).

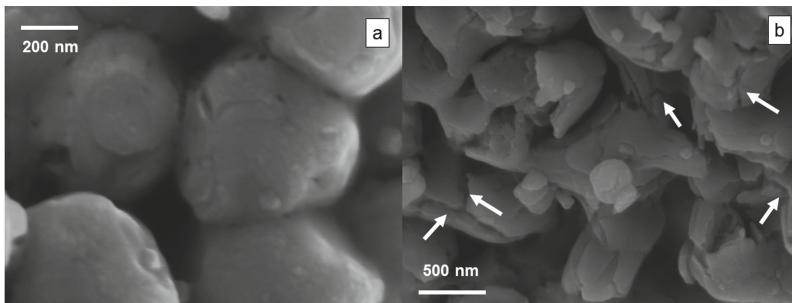


**Fig. 2.** SEM micrographs of steam-slaked portlandite crystals (Tarmac) at high magnification. **b** Arrows highlight nano-cracks due to stress developed during steam slaking.

### 3.3 XRD Analysis

The quantitative analysis of the samples revealed that in the quicklimes less than 5% of the mineral was portlandite, likely due to partial hydration upon contact with moist air

during material handling at the factory or inside the laboratory. Traces of calcite (<1%) were found in the hydrated limes, both water- and steam-slaked (scans of the latter limes shown in Fig. 3), likely due to partial carbonation upon contact with atmospheric moisture and CO<sub>2</sub>, together with traces of aluminum, due to the signal from the sample holder, and zincite, used as internal standard. Apart from these minerals, the analyses showed that all quicklimes are predominantly made of the mineral CaO (i.e. lime), and the hydrated limes are predominantly made of Ca(OH)<sub>2</sub> (i.e. portlandite).

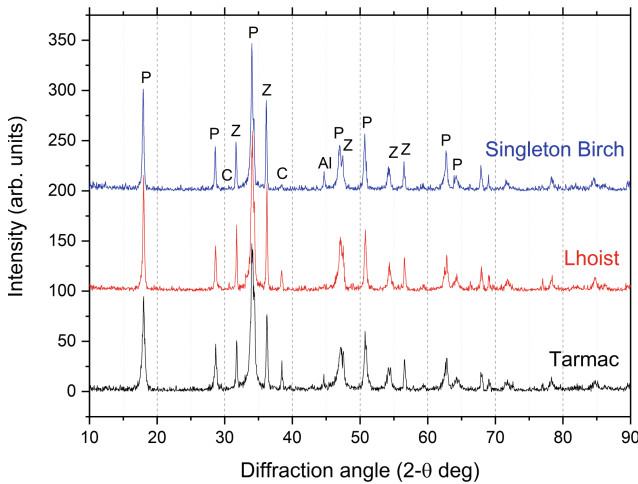


**Fig. 3.** XRD scans of steam-slaked limes (keys: P = portlandite; C = calcite; Z = zincite; Al = aluminum).

In our previous works [5, 18], we showed that the XRD profiles of steam-slaked lime systematically display peaks with a remarkable broadening, when comparing with the same lime slaked in water. The peak broadening is inversely correlated to the crystallite size by the Scherrer's equation, meaning that steam slaked lime has smaller portlandite crystallites. The reduction in crystallite size of steam-slaked lime is likely due to the internal stress developed when portlandite crystals nucleate and grow on the CaO surface and not in solution, as in water-slaked lime [5].

The crystallite size measurements as obtained from the XRD data on the quicklimes and slaked limes are shown in Fig. 4. The graph shows that the quicklimes have a remarkably higher crystallite size (60–70 nm) compared to the hydrated phases. Indeed, it has been previously reported that calcium oxide is a mineral phase of high crystallinity [21–23] and in particular, Brunauer et al. [23] note that there is no significant difference in crystallite size between soft-burned and hard-burned quicklimes. Our results are in agreement with the literature and do not suggest substantial difference in crystallite size across the three manufacturers. Conversely, all the hydrated limes show a small crystallite size (all below 40 nm), suggesting that the slaking results in a hydrated product of lower crystallinity, possibly due to the highly exothermic nature and very fast rate of the hydration reaction. Figure 4 also shows that for the Lhoist and Tarmac samples, the steam slaking leads to a lime with lower crystallite size compared with lime produced through

water slaking. This is likely the consequence of the internal mechanical stress developed during steam-slaking [5], as also suggested by the presence of nano-cracks, visible on the surface of crystals by SEM analysis (Fig. 2b). Remarkably, Singleton Birch lime seems to behave differently, with the crystallite size of the steam-slaked lime only slightly smaller than that of the water-slaked lime. As already observed in the SEM images, the Singleton Birch quicklime displays a different microstructure compared to Lhoist and Tarmac, and such difference is likely to be related to the different characteristics of the geological formation of the parent limestone. It is also worth reporting, to this regard, that during the water slaking it was empirically observed that, whereas Tarmac and Lhoist underwent a very fast, violent hydration reaction which brought the water to a boil in a few seconds from the moment when the water was added, the sample from Singleton Birch took a few minutes before the material started to visibly break, and the overall slaking rate seemed slower than that of the other products. It is likely that the coarser microstructure of the quicklime accounts for its different behaviour on slaking, due to a reduced specific surface area available for reaction. Specific surface area of CaO has been reported to be correlated with hydration rate [23]. A microscopic examination of the limestones used to produce the quicklimes through petrographic analysis and SEM would provide further information on this matter.

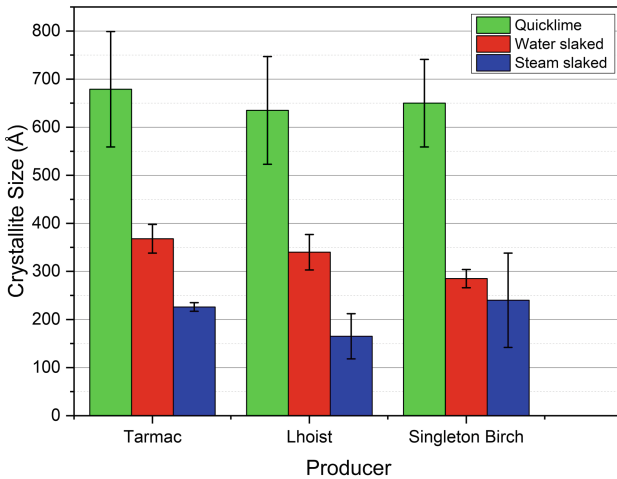


**Fig. 4.** Crystallite size of quicklime, water-slaked hydroxide, and steam-slaked hydroxide from each producer, as calculated by XRD.

## 4 Conclusions

The following conclusions can be drawn from this study:

- The hydrated phases (both water- and steam-slaked) have a much lower crystallinity than the quicklimes, for all three producers;



- The quicklime produced by Singleton Birch has a coarser microstructure in comparison with Tarmac and Lhoist which accounts for a different behaviour on slaking: XRD analyses highlighted that steam-slaked limes from Lhoist and Tarmac have a significantly smaller crystallite size compared to the water-slaked samples. Conversely, Singleton Birch steam-slaked lime shows a crystallite size comparable to that of the water-slaked lime.
- The microstructural differences between Singleton Birch and Tarmac/Lhoist are ascribable to differences in mineralogical characteristics of the parent limestones.
- The reduced crystallinity of steam-slaked lime from Tarmac and Lhoist in comparison with Singleton Birch can be linked to a higher reactivity towards CO<sub>2</sub> and enhanced properties of mortars based on this type of lime.

## References

1. Henry, A.: Hot-mixed mortars: the new lime revival. *Context (Inst. Hist. Build. Conserv.)* **54**, 30–33 (2018)
2. Copsey, N.: *Hot Mixed Lime and Traditional Mortars*. The Crowood Press, Marlborough (2019)
3. Válek, J., Matas, T.: Experimental study of hot mixed mortars in comparison with lime putty and hydrate mortars. *RILEM Bookseries* **7**(September), 269–281 (2013). [https://doi.org/10.1007/978-94-007-4635-0\\_21](https://doi.org/10.1007/978-94-007-4635-0_21)
4. Moropoulou, A., Tsiourva, T., Bisbikou, K., Biscontin, G., Bakolas, A., Zendri, E.: Hot lime technology imparting high strength to historic mortars. *Constr. Build. Mater.* **10**(2), 151–159 (1996)
5. Pesce, C., Godina, M.C., Henry, A., Pesce, G.: Towards a better understanding of hot-mixed mortars for the conservation of historic buildings: the role of water temperature and steam during lime slaking. *Herit. Sci.* **9**(1), 1–18 (2021). <https://doi.org/10.1186/s40494-021-00546-9>
6. Ontiveros-Ortega, E., Ruiz-Agudo, E.M., Ontiveros-Ortega, A.: Thermal decomposition of the CaO in traditional lime kilns. Applications in cultural heritage conservation. *Constr. Build. Mater.* **190**, 349–362 (2018). <https://doi.org/10.1016/j.conbuildmat.2018.09.059>
7. British Standards Institution: Building lime. Definitions, specifications and conformity criteria. BS EN 459-12015 (2015)
8. British Geological Survey: Bee Low Limestone Formation. <https://webapps.bgs.ac.uk/lexicon/lexicon.cfm?pub=BLL>. Accessed 25 Jun 2021
9. British Geological Survey: Welton Chalk Formation. <https://webapps.bgs.ac.uk/lexicon/lexicon.cfm?pub=WCK>. Accessed 25 Jun 2021
10. Tarmac: Cement and Lime Tunstead. <https://tunstead.tarmac.com/cement-and-lime/>. Accessed 24 Jun 2021
11. Tarmac: Environment Tunstead. <https://tunstead.tarmac.com/environment/>. Accessed 24 Jun 2021
12. British Geological Survey: Geology of Britain viewer. <https://www.bgs.ac.uk/map-viewers/geology-of-britain-viewer/>. Accessed 24 Jun 2021
13. Derbyshire County Council and Derby City Council: Derbyshire and Derby Minerals Local Plan (2017). <https://www.derbyshire.gov.uk/site-elements/documents/pdf/environment/planning/planning-policy/minerals-local-plan/industrial-limestone-background-paper.pdf>. Accessed 24 Jun 2021

14. Singleton Birch: Contact us. <https://www.singletonbirch.co.uk/home/contact-us/>
15. Halder, N.C., Wagner, C.N.J.: Separation of particle size and lattice strain in integral breadth measurements. *Acta Crystallogr.* **20**(2), 312–313 (1966). <https://doi.org/10.1107/s0365110x66000628>
16. Witton, T.: Characterization of calcium oxide derived from waste eggshell and its application as CO<sub>2</sub> sorbent. *Ceram. Int.* **37**(8), 3291–3298 (2011). <https://doi.org/10.1016/j.ceramint.2011.05.125>
17. Ginebra, M.P., Driessens, F.C.M., Planell, J.A.: Effect of the particle size on the micro and nanostructural features of a calcium phosphate cement: a kinetic analysis. *Biomaterials* **25**(17), 3453–3462 (2004). <https://doi.org/10.1016/j.biomaterials.2003.10.049>
18. Pesce, C., Pesce, G.: Effects of steam slaking on the characteristics of portlandite crystals. In: *Proceedings of 39th Cement Concrete Science Conference*, pp. 58–61 (2019)
19. Ramachandran, V.S., Sereda, P.J., Feldman, R.F.: Mechanism of hydration of calcium oxide. *Nature* **201**, 288–289 (1964). 1475-2875-9-181[pii]n. <https://doi.org/10.1186/1475-2875-9-181>
20. Beruto, D., Barco, L., Belleri, G., Searcy, A.W.: Vapor-phase hydration of submicrometer CaO particles. *J. Am. Ceram. Soc.* **64**(2), 74–80 (1981). <https://doi.org/10.1111/j.1151-2916.1981.tb09579.x>
21. Fischer, H.C.: Calcination of calcite: II, size and growth rate of calcium oxide crystallites. *J. Am. Ceram. Soc.* **38**(8), 284–288 (1955). <https://doi.org/10.1111/j.1151-2916.1955.tb14946.x>
22. Blanton, T.N., Barnes, C.L.: Quantitative analysis of calcium oxide desiccant conversion to calcium hydroxide using X-ray diffraction. *Adv. X-ray Anal.* **48**, 45–51 (2005). <https://doi.org/10.1154/1.1779815>
23. Brunauer, S., Kantro, D.L., Weise, C.H.: The surface energies of calcium oxide and calcium hydroxide. *Can. J. Chem.* **34**, 729–742 (1956)